

## Simplified Theory of Space-Charge-Limited Currents in an Insulator with Traps

MURRAY A. LAMPERT

*RCA Laboratories, Radio Corporation of America, Princeton, New Jersey*

(Received June 11, 1956)

An ohmic contact between a metal and an insulator facilitates the injection of electrons into the insulator. Subsequent flow of the electrons is space-charge limited. In real insulators the trapping of electrons in localized states in the forbidden gap profoundly influences the current flow. The interesting features of the current density-voltage ( $J-V$ ) characteristic are confined within a "triangle" in the  $\log J-\log V$  plane bounded by three limiting curves: Ohm's law, Child's law for solids ( $J \propto V^2$ ) and a traps-filled-limit curve which has a voltage threshold and an enormously steep current rise. Simple inequalities relating the true field at the anode to the ohmic field facilitate qualitative discussion of the  $J-V$  characteristic. Exact solutions have been obtained for an insulator with a single, discrete trap level in a simplified theory which idealizes the ohmic contact and neglects the diffusive contribution to the current. The discrete trap level produces the same type of nonlinearity discovered by Smith and Rose and attributed by them to traps distributed in energy.

### I. INTRODUCTION

IMPURITY and defect states in insulators profoundly influence their electrical and optical properties. This makes it possible to use these properties to obtain information about the nature of the states. In this study we shall discuss the effect of localized states in an insulator on a particular electrical property, namely the passage of currents limited by space charge.

The reason why space-charge forces play a prominent role in the electrical properties of insulators as compared to, say, semiconductors at room temperature, is that these solids normally have a relatively low density of free carriers and consequently charge unbalance is easily produced by electrical fields. Very large effects can be produced through the use of ohmic contacts which facilitate the direct injection of excess charge into the insulator. The character and magnitude of these effects is due largely to the presence of localized states which can trap and store charge in an equilibrium with the free, mobile charge. The study of space-charge-limited currents can therefore yield such information as the density, location-in-energy and capture cross sections of the trapping states. Finally, the correct interpretation of *any* electrical experiment on insulators requires a proper accounting of the space-charge forces.

Space-charge-limited currents in solids have previously been discussed by Mott and Gurney<sup>1</sup> for a trap-free insulator, by Rose<sup>2</sup> for an insulator with localized trapping states in the forbidden gap, and by Shockley and Prim<sup>3</sup> and Dacey<sup>4</sup> for semiconductors with appropriate  $p-n$  junctions. They have been studied experimentally in insulators by Smith and Rose<sup>5</sup> and in semiconductors by Dacey.<sup>4</sup>

The present study is based on a simplified one dimensional theory which neglects the diffusive contribution to the current and idealizes the ohmic (injecting) contact. The material covered largely complements the pioneering studies of Rose,<sup>2</sup> whose major concern was with electron traps distributed in energy over a region of the forbidden gap. We adopt at the outset a very general point of view in that we specify initially only the minimum amount of detail concerning electron<sup>6</sup> traps in the crystal. We show that the interesting features of the  $J-V$  (current density vs voltage) characteristic are confined within a "triangle" in the  $\log J-\log V$  plane bounded by three limiting curves: Ohm's law ( $J \propto V$ ), Child's law for solids ( $J \propto V^2$ ), and a traps-filled-limit (TFL) curve which has a voltage threshold and an enormously steep current rise. Also we derive simple inequalities relating the true field at the anode to the ohmic field. These inequalities facilitate qualitative discussion of the  $J-V$  characteristic. Exact solutions, within the framework of the simplified theory, are presented for electron traps at a single discrete level. These solutions exhibit the features predicted by the general, qualitative discussion.

Throughout this study the mks system of units is employed. Further, a one-dimensional, plane geometry is adopted for all problems.

### II. BASIS FOR THE SIMPLIFIED THEORY

It is a direct consequence of the energy-band picture for an insulator that an ohmic contact furnishes a reservoir of free electrons which are in the insulator in the region of the contact. This is illustrated in Fig. 1(A) which shows a simplified energy-band diagram for an insulator, with a discrete trap level, in ohmic contact with a metal in thermal and electrical equilibrium. When voltage is applied across the insulator, as in Fig. 1(B), this reservoir will inject electrons into the bulk of the insulator. The metal, in turn, is tightly coupled to

<sup>1</sup> N. F. Mott and R. W. Gurney, *Electronic Processes in Ionic Crystals* (Oxford University Press, New York, 1940), first edition, p. 172.

<sup>2</sup> A. Rose, *Phys. Rev.* **97**, 1538 (1955).

<sup>3</sup> W. Shockley and R. C. Prim, *Phys. Rev.* **90**, 753 (1953).

<sup>4</sup> G. C. Dacey, *Phys. Rev.* **90**, 759 (1953).

<sup>5</sup> R. W. Smith and A. Rose, *Phys. Rev.* **97**, 1531 (1955).

<sup>6</sup> This article is concerned throughout with current flow involving only one sign of carrier. For the sake of definiteness we have taken the carriers to be electrons.

the reservoir and readily replenishes it so long as the current is well below its saturation value for the particular contact at the given temperature. The plot of potential  $V$  vs position  $x$  in Fig. 1(B) exhibits the minimum which is characteristic of space-charge-limited currents.

The exact theory is based on three equations—a current flow equation, Poisson's equation, and an equation of state relating the free-electron density to the trapped-electron density at the same position. With the sign conventions,

$$\mathbf{J} = -J\mathbf{x}, \quad \mathcal{E} = -\mathcal{E}\mathbf{x}, \quad \mathcal{E} = dV/dx,$$

these equations are, respectively:

$$J = e\mu n\mathcal{E} - eD(dn/dx) = \text{constant}, \quad (1')$$

$$(\epsilon/e)(d\mathcal{E}/dx) = (n - \bar{n}) + (n_t - \bar{n}_t), \quad (2)$$

$$n \text{ and } n_t \text{ are in quasi-thermal equilibrium}, \quad (3)$$

where  $\mathbf{J}$  is the current density;  $J = |\mathbf{J}|$ ;  $\mathcal{E}$  is the electric field intensity;  $\mathcal{E} = |\mathcal{E}|$ ;  $e$  is the magnitude of the electronic charge;  $\mu$  is the electronic mobility;  $D$  is the diffusion constant for electrons;  $\epsilon$  is the static dielectric constant of the insulator;  $n$  and  $n_t$  are the densities of free and trapped electrons, respectively; they are functions of position  $x$ ;  $\bar{n}$  and  $\bar{n}_t$  are the values of  $n$  and  $n_t$ , respectively, in the bulk neutral crystal in thermal and electrical equilibrium (no applied voltage).

The "quasi-thermal equilibrium" of (3) is a shorthand way of stating that the steady-state Fermi level  $F(x)$ , defined with reference to  $n(x)$ , determines the occupancy of the electron traps via the usual Fermi-

Dirac occupation function.  $F(x)$  is given by<sup>7</sup>

$$n(x) = N_c \exp\{[F(x) - E_c(x)]/kT\}, \quad (4)$$

where  $N_c$  is the effective density of states<sup>8</sup> in the conduction band at temperature  $T$  and  $E_c(x)$  is the electron energy at the conduction band minima at position  $x$ .

A set of traps of density  $N_t$  at energy  $E_t(x)$  are, in quasi-thermal equilibrium with  $n(x)$ , occupied according to<sup>9</sup>

$$n_t(x) = N_t \left\{ 1 + \exp\left(\frac{E_t(x) - F(x)}{kT}\right) \right\}^{-1} \\ = n(x)N_t\{n(x) + N\}^{-1}, \quad (5)$$

with

$$N = N_c \exp\{[E_t(x) - E_c(x)]/kT\}.$$

The solution of Eqs. (1')–(3) requires specification of a pair of boundary conditions. It is convenient to consider the insulator as a semi-infinite crystal, thus in Fig. 1, extended to  $x = \infty$ . In Eq. (2),  $\bar{n}$  and  $\bar{n}_t$  are then taken at  $x = \infty$ . One of the two boundary conditions is simply<sup>10</sup>:

$$(\text{boundary condition}) \quad n(x) \rightarrow \bar{n} \text{ as } x \rightarrow \infty. \quad (6)$$

From Eq. (3) it follows that  $n_t(x) \rightarrow \bar{n}_t$  as  $x \rightarrow \infty$ .

The second boundary condition must be specified at the interface,  $x=0$  in Fig. 1.

The system of equations (1')–(3), with the electron traps specified, can be reduced to a nonlinear second-order differential equation in the free-carrier density  $n(x)$ . It appears to be very difficult, and perhaps impossible, to obtain, in terms of known functions an analytic solution of this equation obeying the boundary condition (6). Also there are difficulties and uncer-

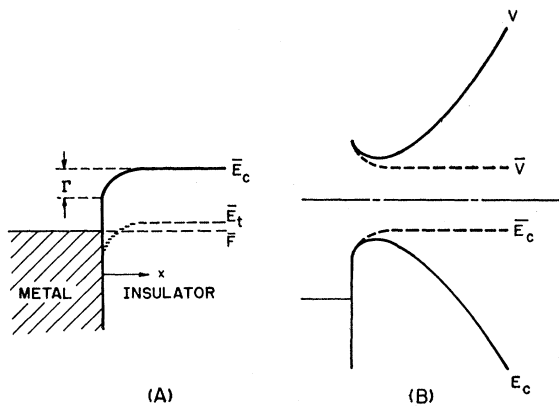


FIG. 1. Simplified energy-band diagrams for an injecting contact of an insulator with a metal. (A): The contact in thermal and electrical equilibrium.  $\bar{F}$  is the thermodynamic Fermi level,  $\bar{E}_t$  a single, discrete trap level, and  $\bar{E}_c$  the bottom level of the conduction band.  $\bar{E}_t$  and  $\bar{E}_c$  are functions of position  $x$ . The amount  $\Gamma$  of downward-bending of the bands at the contact is, in a simplified picture neglecting surface influences, given by the difference of work functions of the insulator and metal:  $\Gamma = \Phi_I - \Phi_M$ . The density of electrons in the conduction band at position  $x$ ,  $\bar{n}(x)$ , is given by:  $\bar{n}(x) = N_c \exp\{[\bar{F} - \bar{E}_c(x)]/kT\}$ ,  $N_c$  being the effective density of conduction-band states at temperature  $T$ . The slanted solid lines denote the Fermi sea of electrons in the metal. (B): The contact in steady state under an applied voltage.  $V$  is the electric potential,  $E_c$  the total free-carrier energy (both solid lines). The corresponding thermodynamic equilibrium quantities,  $\bar{V}$  and  $\bar{E}_c$ , are indicated by dashed lines.

<sup>7</sup> Here, for the sake of convenience, we are assuming non-degeneracy of the electrons in the conduction band, even under current flow. For insulators this will certainly be the usual situation.

<sup>8</sup> See, e.g., W. Shockley, "Electrons and Holes in Semiconductors" (D. Van Nostrand Company, Inc., New York, 1950), p. 240.

<sup>9</sup> The criterion for the validity of the assumption of quasi-thermal equilibrium as written in (5), is that  $\langle e_n \rangle / \langle c_n \rangle = \exp\{-(E_t - E_c)/kT\}$ . Here  $\langle e_n \rangle$  is the probability per unit time of thermal ejection of an electron from an occupied trap into the conduction band and  $\langle c_n \rangle = \langle v\sigma_n \rangle$  is the probability per unit time of capture of an electron from the conduction band into an unoccupied trap,  $v$  being the velocity of the electron and  $\sigma_n$  the cross section for its capture by the trap.  $\langle \rangle$  denotes, in each case, the proper average over the conduction band states. This criterion will be met under quite general conditions. However, if the electric field intensity is high enough to "heat up" the electrons to a temperature  $T_e$  substantially exceeding the lattice temperature  $T$  and if  $\sigma_n$  is strongly velocity dependent, then the condition will not be met since  $\langle e_n \rangle$  will be essentially equal to its thermal and electrical equilibrium value,  $\langle \bar{e}_n \rangle$ , whereas  $\langle c_n \rangle$  will differ substantially from its equilibrium value,  $\langle \bar{c}_n \rangle$ .

<sup>10</sup> For a finite crystal with the anode contact at  $x=a$ , it is assumed simply that the solution for the semi-infinite crystal holds undisturbed up to the point  $x=a$ . This is generally the procedure followed in the treatment of this type of problem, and underlying it is clearly the assumption, usually left implicit, that the anode does not itself introduce constraints into the problem. This assumption is made also in the "simplified theory" discussed in this article.

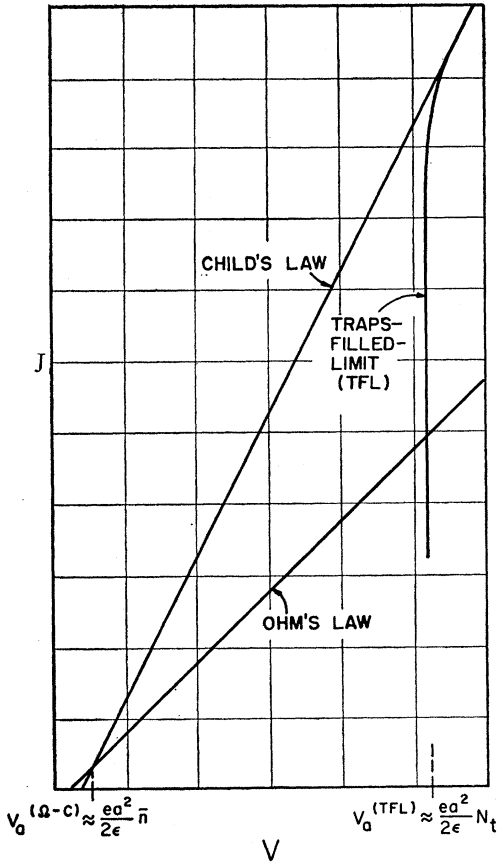


FIG. 2. Log-log plot of limiting current density ( $J$ ) versus voltage ( $V$ ) characteristics for space-charge-limited currents in an insulator with traps.

tainties, related to the physics of the interface in establishing the appropriate boundary condition at  $x=0$ . An analytic solution has been given by Shockley and Prim<sup>3</sup> for the simplest possible problem of this type, namely with  $\bar{n}=0$ ,  $\bar{n}_i=0$ ,  $n_i \equiv 0$  in Eq. (2). Even in this case the solution is quite complicated. Their solution is not useful for our present study because it omits all trapping effects.

In order to obtain a picture of the space-charge-limited currents in an insulator, we have followed the procedure of replacing the current flow equation (1') by the simpler equation obtained by neglecting the diffusive contribution to the current. Thus (1') is replaced by

$$J = en\mu\mathcal{E} = \text{constant.} \quad (1)$$

With this simplification the boundary condition appropriate for the description of space-charge-limited currents is

$$\text{(boundary condition) } \mathcal{E} = 0 \text{ at } x = 0 \text{ (the cathode interface).} \quad (7)$$

Equations (1), (2), and (3) and the boundary condition (7) provide the mathematical framework for the

"simplified theory" of space-charge-limited currents in an insulator. The boundary condition (7) coupled with Eq. (1) requires that  $n$  be infinite at the cathode interface.

A discussion of the range of application of the simplified theory is given in Sec. V.

### III. LIMITING CURRENT DENSITY-VOLTAGE CHARACTERISTICS. LOG $J$ -LOG $V$ "TRIANGLE"

An over-all view of the obtainable  $J$ - $V$  characteristics can be obtained by an examination of certain limiting cases of current flow. In Fig. 2 is shown a log-log plot of current density  $J$  vs voltage  $V$  for three such cases.

The lower curve is Ohm's law for the neutral crystal,  $J_\Omega = e\bar{n}\mu\mathcal{E}_\Omega$ , where  $\mathcal{E}_\Omega$  is the ohmic electric field intensity,  $\mathcal{E}_\Omega = V_a/a$ , with  $a$  the cathode-anode spacing and  $V_a$  the applied voltage.

The upper curve is Child's law for solids,  $J_c = 9\epsilon\mu V_a^2/8a^3$ , valid for a trap-free crystal,  $\bar{n}_i=0$ ,  $n_i \equiv 0$ , with a negligible "dark density" of carriers,  $\bar{n} \approx 0$ . It is obtained by direct integration of Eqs. (1) and (2) using boundary condition (7).

The Ohm's law and Child's law curves intersect at the voltage  $V_a^{(\Omega-c)} = 8ea^2\bar{n}/9\epsilon$ . This crossover occurs when the excess injected carrier density at the anode, calculated from Child's law, reaches the same magnitude as the dark density  $\bar{n}$ .

The curve on the right, labeled traps-filled-limit or TFL, is the curve corresponding to the situation that the traps in the crystal have all been filled prior to the application of voltage. We note that there is a voltage threshold, denoted by  $V_a^{(TFL)}$ , for current flow. This is due to the fact that before voltage is applied there is already unneutralized charge in the traps which prevents the injection of additional electrons at the cathode. The voltage  $V_a^{(TFL)} = ea^2N_t/2\epsilon$ , with  $N_t$  the total trap density, is necessary to overcome this repulsion. The enormous steepness of the TFL curve relative to the Ohm's law curve, as exhibited in Fig. 2, follows only on the assumption that the trap density  $N_t$  greatly exceeds the dark density  $\bar{n}$ . Indeed the ratio of the slope  $\Delta_{TFL}$  of the TFL curve to that,  $\Delta_\Omega$ , of the Ohm's law curve at their point of intersection is  $\Delta_{TFL}/\Delta_\Omega \approx N_t/\bar{n}$ . The TFL curve is practically vertical, for  $N_t/\bar{n} \gg 1$ , up to a decade or so below its extrapolated intersection with the Child's law curve.

A mathematical treatment of the TFL law is given in Appendix A. The mathematics of the transition, in a trap-free crystal, from Ohm's law to Child's law is also presented in Appendix A. The solution given there also yields a correction to Child's law.

It is possible to state at the outset some quite general properties of the true current density-voltage characteristic in the real crystal with traps in relation to the "triangle" of Fig. 2.

(i) The true  $J$ - $V$  curve cannot lie below the Ohm's law line. For the reservoir of electrons at the cathode

can only have added, through injection, additional carriers to those already present thermally.<sup>11</sup>

(ii) The true  $J-V$  curve cannot lie above the Child's law line, for voltages at which a significant amount of carrier injection takes place, i.e., for  $V_a > V_a^{(\Omega-C)}$ . For this represents the case that *all* of the excess, injected charge in the insulator, corresponding to a given applied voltage, is in the conduction band. If any of this injected charge is trapped, then the current must be correspondingly lower.

(iii) The true  $J-V$  curve cannot lie below the TFL curve; i.e., it cannot lie to the right of this limit. For this limit represents the most unfavorable situation, current-wise, namely one in which the greatest possible fraction of excess charge in the insulator is trapped, and therefore the smallest fraction is available for conduction.

Therefore the following conclusions may be drawn about the behavior of the true  $J-V$  curve.

At voltages below the Ohm's law—Child's law crossover,  $V_a^{(\Omega-C)}$ , the true curve follows Ohm's law.

Above  $V_a^{(\Omega-C)}$  the true curve lies somewhere inside the "triangle". At voltage  $V_a^{(TFL)}$ , if the true  $J-V$  curve lies sufficiently below Child's law curve, it will merge with the vertical portion of the TFL curve.

At higher voltages, where the TFL merges with Child's law, namely somewhat above  $V_a^{(TFL)}$  (by about 50%), the true  $J-V$  curve follows Child's law.

Since all of the possible nonlinearities of interest in the true  $J-V$  curve must lie inside the "triangle" of Fig. (2), it is useful to know the size of this "triangle". The key quantity determining this size is the ratio  $V_a^{(TFL)}/V_a^{(\Omega-C)} \approx N_t/\bar{n}$ . With trap densities  $N_t \gtrsim 10^{14}$  cm<sup>-3</sup> being the rule for insulators in the current state of their technology, there will obviously be plenty of "room" available for nonlinearity.

#### IV. USEFUL INEQUALITY, SOME SIMPLIFICATIONS IN REASONING, AND SOME CALCULATED RESULTS

Without actually solving Eqs. (1)–(3), some further detailed information, beyond that of Sec. III, can be obtained with the help of general arguments.

An important simplification results from the observation that the electric field intensity at the anode,  $\mathcal{E}_a$ , is not very different in magnitude from the "ohmic" field intensity  $\mathcal{E}_\Omega = V_a/a$ . Indeed, we establish rigorously the inequality<sup>12</sup>

$$\mathcal{E}_\Omega < \mathcal{E}_a < 2\mathcal{E}_\Omega. \quad (8)$$

<sup>11</sup> A formal proof that  $n(x) > \bar{n}$  for all  $x$ , in Eq. (2), is easily provided:  $n = \infty$  at  $x=0$ . If  $n(x) < \bar{n}$  at some  $x$  there must be a first crossing point, say at  $x_1$ ,  $n(x_1) = \bar{n}$ . Immediately beyond  $x_1$ ,  $n(x) < \bar{n}$  whence also, from Eqs. (2) and (3),  $d\mathcal{E}/dx < 0$ . But  $n(x)$  and  $\mathcal{E}(x)$  simultaneously decreasing is inconsistent with Eq. (1), and the assumption of a crossing has produced a contradiction.

<sup>12</sup> Rose (reference 2) employs throughout his work the relation  $Q_{tot} = CV_a$ , where  $Q_{tot}$  is the total injected, excess charge in the insulator per unit cross-sectional area and  $C$  is taken as the capacitance per unit area of the electrode-insulator combination. For a plane-parallel geometry, this capacitance is  $\epsilon/a$  (mks units). The inequality (8) is equivalent, for this geometry, to the inequality

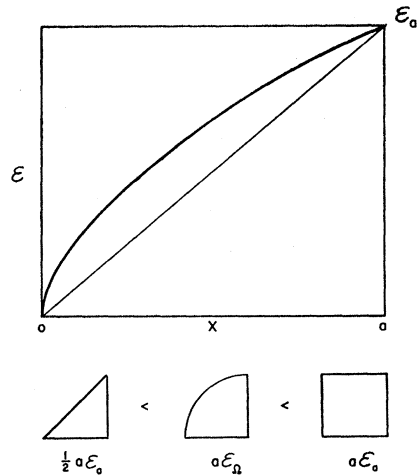


FIG. 3. Convexity of the electric field intensity distribution  $\mathcal{E}$  and consequent inequalities. The quantities under the geometric figures are the areas of the corresponding figures.

We have already seen (footnote 11) that everywhere throughout the crystal  $n > \bar{n}$  and  $n_i > \bar{n}_i$ . Hence, from Eq. (2),  $d\mathcal{E}/dx > 0$  and  $\mathcal{E}$  increases monotonically from zero at the cathode. Therefore, from Eqs. (1) and (3),  $n$  and  $n_i$  must both decrease monotonically going out from the cathode. Hence from Eq. (2),  $d\mathcal{E}/dx$  decreases monotonically from infinity at the cathode. Finally, a plot of  $\mathcal{E}$  vs  $x$  must have the convex shape indicated in Fig. 3. But a comparison of the three areas, as in Fig. 3, yields immediately the inequalities:  $\mathcal{E}_a/2 < \mathcal{E}_\Omega < \mathcal{E}_a$  which are equivalent to (8). For Child's law,  $\mathcal{E}_a = 3\mathcal{E}_\Omega/2$ . Over the "vertical" portion of the traps-filled-limit law in Fig. 2,  $\mathcal{E}_a \approx 2\mathcal{E}_\Omega$ . [See (A15) of Appendix A.]

Noting, from Eq. (1), that  $J/J_\Omega = n(x)\mathcal{E}(x)/\bar{n}\mathcal{E}_\Omega = n_a\mathcal{E}_a/\bar{n}\mathcal{E}_\Omega$ , then, within a factor of two, the following relations are valid:

$$J/J_\Omega \approx n_a/\bar{n}, \quad J \approx en_a\mu\mathcal{E}_\Omega. \quad (9)$$

Here we have the first important simplification: The current density can be estimated simply by determining the free-carrier density at the anode, or equivalently, the position of the steady-state Fermi level at the anode.

To relate  $J$  directly to  $V_a$ , it remains to relate  $n_a$  to  $V_a$ . Integration of Eq. (2) under boundary condition (7) gives:  $\epsilon\mathcal{E}_a/ea = (n_\Omega - \bar{n}) + (n_{i\Omega} - \bar{n}_i)$ , with  $n_\Omega = (1/a) \times \int_0^a n(x)dx$  and  $n_{i\Omega} = (1/a) \int_0^a n_i(x)dx$ . We now make the assumption that  $n_a \approx n_\Omega$  and  $n_{ia} \approx n_{i\Omega}$ . It would be most desirable to set quite general and relatively narrow limits, along the lines of (8), on the maximum error incurred by these assumptions. Unfortunately the traps-filled-limit case provides a counter-example to show that this is impossible [see (A16) of Appendix A]. Nevertheless, the discussion in Appendix A leads us to expect that relatively small errors are incurred by these assumptions. Replacing  $n_\Omega$  by  $n_a$ ,  $n_{i\Omega}$  by  $n_{ia}$ , and  $\mathcal{E}_a$  by

ity  $\epsilon/a < C < 2\epsilon/a$ , and therefore Rose's assumption involves an error of at most a factor of two.

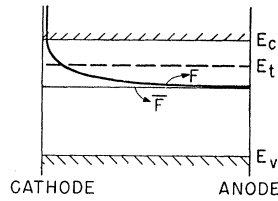


FIG. 4. Relative plot of the steady-state Fermi level  $F$  for a given current flow in an insulator with a single, discrete trap level  $E_t$ .

$V_a/a$  in the above equation gives

$$\epsilon V_a / ea^2 \approx (n_a - \bar{n}) + (n_{ta} - \bar{n}_t). \quad (10)$$

Combining (9) with (10) gives the desired relationship between  $J$  and  $V_a$ . To be sure, it is first necessary to relate  $n_a$  to  $n_{ta}$ , but in practice, once the energy distribution of traps within the forbidden gap is known, this is done very simply.

To illustrate the usefulness of the simplified approach developed above we apply it to a case of particular interest, namely that in which the traps are located at a single, discrete energy level in the forbidden gap.

This case is illustrated in Fig. 4 where the location of the steady-state Fermi level with respect to the energy bands is plotted *versus* position for a given current flow. Actually the energy bands should be drawn tilted, as in Fig. 1(B), due to the applied voltage, but since our interest is in the *relative* location of  $F$ , we have drawn the energy bands horizontal. According to the above arguments, the over-all features of the current density-voltage characteristic can be determined by fixing our attention on the location in energy of  $F_a$ , the steady-state Fermi level at the anode.

So long as  $F_a$  lies below the trap level  $E_t$  there is a fixed ratio  $\theta$ , *independent of applied voltage*, between  $n_a$  and  $n_{ta}$ :

$$\left( \frac{E_t - F_a}{kT} > 1 \right) : \frac{n_a}{n_{ta}} = \theta = \frac{N_c}{N_t} \exp \left( \frac{E_t - E_c}{kT} \right). \quad (11)$$

Thus, of the total charge density at the anode end only the fraction  $\theta$  is available for conduction (assuming, here, that  $\theta \ll 1$ ). Since the effectiveness of the dark density  $\bar{n}$  of free carriers relative to the injected free carriers is greater by the factor  $1/\theta$  over their trap-free effectiveness, the transition voltage marking the departure from Ohm's law will likewise be a factor  $1/\theta$  greater than the trap-free transition voltage  $V_a^{(\Omega-c)}$  of Fig. 2. Thus the  $J-V$  characteristic will follow Ohm's law up to the voltage  $V_{\theta, a}^{(\Omega-c)} \approx ea^2 \bar{n} / 2e\theta$ .

For  $V_a^{(\text{TFL})} > V_a > V_{\theta, a}^{(\Omega-c)}$ ,  $F_a$  lies below  $E_t$  and the  $J-V$  characteristic follows Child's law for solids modified by the correction factor  $\theta$ :  $J = 9\theta\epsilon\mu V_a^2 / 8a^3$ .

At  $V_a \approx V_a^{(\text{TFL})}$  the traps fill and the  $J-V$  characteristic thereafter follows the traps-filled-limit law and finally the full Child's law.

This same method of reasoning is easily generalized

to cover more complicated cases, such as several discrete trap levels or distributions of trap levels.

Exact analytic solutions have been obtained, within the framework of the simplified theory, for the case of a single, discrete trap level. These solutions, which are presented in Appendix C, have been plotted graphically in Fig. 5 using constants corresponding to a cadmium sulfide crystal of high purity and convenient dimension for experimental study. It is seen that the various curves corresponding to different choices of trap depth  $G = E_c - E_t$ , follow the above-predicted behavior. It is to be noted that the curve corresponding to  $G = 0.7$  ev becomes vertical at a voltage smaller than the  $V_a^{(\text{TFL})}$  for the other curves, corresponding to the dashed vertical line. The reason is (see Appendix A) that the threshold voltage is accurately given by  $V_a^{(\text{TFL})} = ea^2 \times (N_t - \bar{n}_t - \bar{n}) / 2e$ . For  $E_c - \bar{F} = 0.75$  ev and  $G = 0.7$  ev,  $N_t - \bar{n}_t - \bar{n} = 0.865N_t$ , whereas for  $G \leq 0.6$  ev,  $N_t - \bar{n}_t - \bar{n} \approx N_t$ .

The ratio of the slopes  $\Delta_{\theta, c} = dJ/dV$  of a modified Child's law curve and  $\Delta_{\theta, \text{TFL}}$  of the traps-filled-limit curve at their (extrapolated) point of intersection is  $\Delta_{\theta, \text{TFL}} / \Delta_{\theta, c} \approx 1/\theta$  with  $\theta$  given by (11). This change of slope is so great that, if encountered in practice, would,

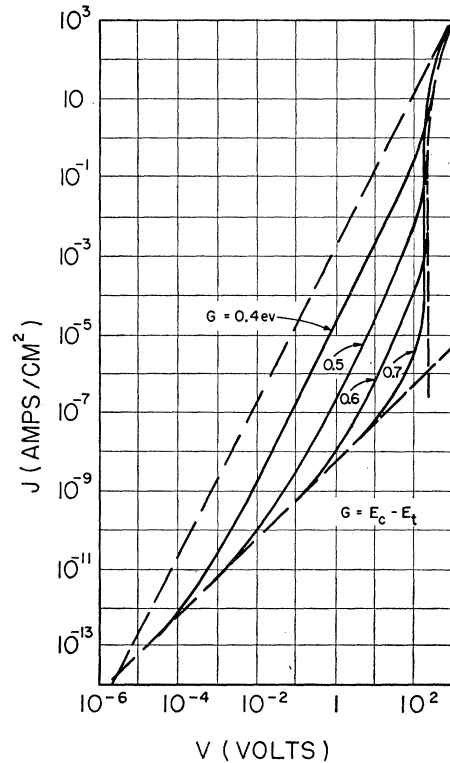


FIG. 5. Exact solutions for the simplified theory of space-charge-limited currents in a CdS crystal with traps at a single, discrete energy level. The dashed curves are the three limiting characteristics of Fig. 2. For CdS,  $\epsilon/\epsilon_0 = 11$ , and  $\mu = 200$  cm<sup>2</sup>/volt sec at  $T = 300^\circ\text{K}$ . The solid curves are the calculated solutions; for all curves  $N_t = 10^{14}$  cm<sup>-3</sup>,  $a = 5 \times 10^{-3}$  cm,  $E_c - \bar{F} = 0.75$  ev, corresponding to  $\bar{n} \approx 10^6$  cm<sup>-3</sup> and resistivity  $\rho \approx 3 \times 10^{10}$  ohm cm at  $T = 300^\circ\text{K}$ .

prior to Rose's work,<sup>2</sup> surely have been misinterpreted as an electronic breakdown. Comparing the current density  $J^{(\text{ONSET})}$  at the onset of the almost vertical portion of the  $J-V$  characteristic to that,  $J^{(\text{EXIT})}$ , at the exit from this portion of the curve, we find that the range of "verticality" is  $J^{(\text{EXIT})}/J^{(\text{ONSET})} \approx 1/\theta$ .

### V. CONCLUDING REMARKS

Both theoretically and experimentally much work remains to be done on space-charge-limited currents in insulators.

On the theoretical side it would be desirable to obtain a quantitative estimate of the errors incurred by using the simplified theory in place of the more accurate theory characterized by Eq. (1'), boundary condition (6) and another (unspecified) boundary condition at the cathode. Clearly the solutions of the simplified theory are completely in error in the immediate vicinity of the cathode interface, since for all such solutions  $n = \infty$  and  $dn/dx = -\infty$  at  $x=0$ . Nonetheless, at currents which are space-charge limited, that is, for which the potential minimum of Fig. 1(B) has not yet moved past the interface, we will expect that far enough away from the interface the solutions of the simplified theory are actually quite accurate. If the region near the interface where the diffusion current exceeds or is comparable to drift current is of extent  $l(J)$ , then at a distance  $L$  from the interface, where  $L \gg l(J)$ , the solution of the simplified theory should not be in error by more than the factor  $1 + K[l(J)/L]$ , where  $K$  will be on the order of two or less. This follows simply from the functional form of the solutions in the Child's law case, the trap-filled-limit case, etc. Beyond these general remarks, a detailed evaluation of the errors in the solutions of the simplified theory can only be obtained if the comparable solutions of the accurate theory are also worked out. For the one case in which the solutions have been obtained for both theories, namely the trap-free insulator with no free carriers in the dark, the above remarks are borne out by the calculations.<sup>13</sup>

The simplified theory, by its very nature, fails to give any information whatever on the onset of saturation, that is the point at which the potential minimum moves past the interface and out of the insulator. Beyond this point, the current is no longer completely space-charge-limited. This region of the  $J-V$  characteristic can be studied only by invoking the more accurate theory in conjunction with a reasonably realistic picture of the contact. Where the currents are well into the saturation region, a simplified theory can again be invoked with the boundary condition (7) replaced by a new boundary condition related to the detailed electronic structure of the contact.

On the experimental side, the work of Smith and Rose<sup>5</sup> has provided abundant evidence for the existence of space-charge-limited currents in an insulator with traps, namely in CdS. In particular they have confirmed

<sup>13</sup> See reference 3, Fig. 5 on p. 756.

Child's law for solids by pulse measurements. They have also measured extremely nonlinear steady-state currents<sup>14</sup> which they attribute to traps distributed in energy in the forbidden gap. A more quantitative check of theory with experiment can perhaps be obtained through study of an insulator with a known density of traps at a single, discrete trap level. The two solids whose advanced state of technology make particularly suitable candidates for such a study are germanium and silicon. In a compensated sample with  $N_d$  donors/cm<sup>3</sup> and  $N_A$  acceptors/cm<sup>3</sup> with  $N_d > N_A$ , at a temperature low enough to condense most of the free carriers back on the parent donors, and with  $N_A \gg \bar{n}$ , there will be  $N_A$  electron traps/cm<sup>3</sup>, at the known donor level. For germanium with hydrogenic-type (Group V) donors, the experiment would have to be done at liquid-helium temperature, and the results being sought would likely be swamped by low-field breakdown. (However, carrier injection under conditions of space-charge-limitation *might* make itself felt in the prebreakdown current region.<sup>15</sup>)

Use of germanium doped with a nonhydrogenic type of impurity offers the possibility of an experiment at liquid air temperature. An example might be gold-doped germanium, although here the double-acceptor state of the gold would necessitate carefully-controlled compensation. Silicon, suitably doped, also offers the possibility of a critical experiment at liquid air temperature.

The author would here like to express his considerable indebtedness to Dr. H. S. Sommers, Jr., Dr. A. Rose, Mr. R. W. Smith, Dr. L. Nergaard, and Dr. D. O. North for many stimulating and helpful discussions. The general lines of reasoning employed in the present study were first developed by Dr. Rose and indeed form the intuitive basis for his earlier studies in this field.

### APPENDIX A. MATHEMATICAL SOLUTIONS FOR A TRAP-FREE INSULATOR AND A TRAP-FILLED INSULATOR

The solutions of Eqs. (1) and (2) for the two limiting cases of a trap-free crystal and a trap-filled<sup>16</sup> crystal follow almost identical lines and so may be discussed together. Equation (2) may be written

$$(\epsilon/e)(d\mathcal{E}/dx) = n - \bar{n};$$

$$\begin{cases} \text{upper sign for the trap-free crystal } (\bar{n} = \bar{n}) \\ \text{lower sign for the trap-filled crystal } (\bar{n} = N_t - \bar{n}_t - \bar{n}). \end{cases} \quad (\text{A1})$$

<sup>14</sup> See reference 5, Fig. 4 on p. 1534, curve labeled I and the discussion on p. 1534.

<sup>15</sup> This possibility was pointed out by R. Bray (private communication).

<sup>16</sup> The equivalent of the trap-filled case has previously been studied by Shockley and Prim (see reference 3, p. 754) in connection with certain semiconductor problems. However, their entire discussion, including their choice of normalized variables, centers around particular types of transistor structures and consequently the detailed form of their solution, (2.7) through (2.15), p. 755, is unsuitable for discussion of the insulator problem.

It is convenient to obtain the solutions in terms of dimensionless distance, field, and potential variables  $w$ ,  $u$ , and  $v$ , respectively, defined as follows:

$$w = e^2 \tilde{n}^2 \mu x / \epsilon J, \quad u = e \tilde{n} \mu \mathcal{E} / J = \tilde{n} / n, \quad v = e^3 \tilde{n}^3 \mu^2 V / \epsilon J^2. \quad (A2)$$

The current Eq. (1) has been used in (A2) in expressing  $u$  as a ratio of carrier densities.

The Poisson equation (A1) becomes

$$du/dw = (1/u) \mp 1, \quad (A3)$$

and the definition of the potential,  $V(x) = \int_0^x \mathcal{E}(x) dx$ , becomes

$$v = \int_0^u u \frac{dw}{du} du = \int_0^u \frac{u^2}{1 \mp u} du. \quad (A4)$$

The integration of Eqs. (A3) and (A4), subject to the boundary condition (7):  $u=0$  at  $w=0$ , gives

$$w = \mp u - \ln(1 \mp u), \quad (A5)$$

$$v = \mp \frac{1}{2} u^2 - u \mp \ln(1 \mp u). \quad (A6)$$

The range of  $u$  is from  $u=0$  at  $w=0$  to  $u=1$  at  $w = \infty$  for the upper sign, and for the lower sign, to  $u = \infty$  at  $w = \infty$ .

It would be desirable to obtain  $u$  and  $v$  as explicit "simple" functions of  $w$ , but inspection of (A5) and (A6) shows that this is clearly impossible over the entire range of  $w$ , although it is a simple matter over limited ranges of  $w$  at its extremes, as is done below. In this respect, these relatively simple limiting cases exhibit a basic feature which appears almost universally throughout the entire class of problems of space-charge-limited current flow with one sign of carrier. Namely it is, with the exception of the Child's law case,<sup>17</sup> [ $\tilde{n}=0$  in Eq. (A1)] (without or with the inclusion of the diffusion current) apparently impossible to obtain explicit solutions in closed form in terms of known functions.

Further, the form of the solution, namely Eqs. (A5) and (A6), is also typical of what one encounters generally, as seen in Appendix C following.

The solutions of Eqs. (A5) and (A6) are, for  $w$  small and  $w$  large, respectively:

$$w \ll 1: \quad u \simeq (2w)^{\frac{1}{2}}, \quad v \simeq \frac{1}{3} (2w)^{\frac{3}{2}}; \quad (A7)$$

$$w \gg 1: \quad \begin{cases} \text{upper sign: } u \simeq 1 - e^{-w}, & v \simeq w; \\ \text{lower sign: } u \simeq w, & v \simeq \frac{1}{2} w^2. \end{cases} \quad (A8)$$

For the further discussion of the problem, it is convenient to define an ohmic field intensity  $\mathcal{E}_0$ , an ohmic-like current density  $J_0$  and a dimensionless voltage parameter  $\alpha$  as follows:

$$\mathcal{E}_0 = V_a/a, \quad J_0 = e \tilde{n} \mu \mathcal{E}_0, \quad \alpha = \epsilon V_a / e \tilde{n} a^2 = v_a / w_a^2, \quad (A9)$$

where subscript "a" denotes the value of a quantity at the anode,  $x=a$ . With  $\alpha$  (i.e., the applied voltage  $V_a$ ) given,  $v_a$ ,  $w_a$ , and  $u_a$  are to be determined, and from

<sup>17</sup> See reference 3 for the explicit solutions in this case.

these in turn are obtained the values of all physical quantities of interest. Where analytic approximations cannot be used, a useful procedure is to plot graphically, using Eqs. (A5) and (A6), the ratio  $v/w^2$  vs  $u$ . This ratio decreases monotonically from  $\infty$  at  $u=0$  to 0 at  $u=1$  for the upper sign, and to  $\frac{1}{2}$  at  $u = \infty$  for the lower sign. With  $\alpha$  given, this plot enables us to determine uniquely the corresponding value of  $u_a$ . The values of  $w_a$  and  $v_a$  are then obtained from Eqs. (A5) and (A6), respectively. For the resulting current density  $J$ , free-carrier density at the anode  $n_a$ , and field intensity at the anode  $\mathcal{E}_a$ , we have the relations, obtained from (A2):

$$J/J_0 = w_a/v_a, \quad n_a/\tilde{n} = 1/u_a, \quad \mathcal{E}_a/\mathcal{E}_0 = u_a w_a/v_a. \quad (A10)$$

The field intensity, free-carrier density, and potential distributions along the insulator are conveniently obtained from Eqs. (A5) and (A6) via the scaling relations.

$$x/a = w/w_a, \quad \mathcal{E}(x)/\mathcal{E}_a = n_a/n(x) = u/u_a, \quad V(x)/V_a = v/v_a. \quad (A11)$$

For  $\alpha$  greater than unity,  $u_a \ll 1$  and expansion of  $\ln(1 \mp u)$ , in (A5) and (A6), as a power series in  $u$  leads, via the approximations (A7) including higher order terms, to the analytic approximations

$$\frac{J}{J_0} \simeq \frac{9}{8} \alpha \pm \frac{3}{4}; \quad \frac{n_a}{\tilde{n}} \simeq \frac{3}{4} \alpha \pm \frac{7}{12}; \quad \frac{\mathcal{E}_a}{\mathcal{E}_0} \simeq \frac{3}{2} \mp \frac{1}{6\alpha}. \quad (A12)$$

This is the Child's law region of current; indeed the relation  $J/J_0 = 9\alpha/8$  is exactly Child's law. The approximations (A12) are very accurate for  $\alpha \geq 1$  and quite fair for  $0.7 < \alpha < 1$ . Note that  $\alpha=1$  corresponds to a voltage equal to twice  $V_a^{(Q-C)}$  for the trap-free crystal and to twice  $V_a^{(TFL)}$  for the trap-filled crystal.

Beyond this point it is convenient to discuss the two cases separately.

(i) *The trap-free crystal; Ohm's law and the Ohm's law-Child's law transition.*—For  $\alpha \ll 1$ ,  $u_a$  is very close to unity, and the following analytic approximations are useful:

$$\frac{J}{J_0} \simeq 1 + \frac{1}{2} \alpha; \quad \frac{n_a}{\tilde{n}} \simeq 1 + \left[ \exp - \left( \frac{1}{\alpha} + 1 \right) \right]; \quad \frac{\mathcal{E}_a}{\mathcal{E}_0} \simeq 1 + \frac{1}{2} \alpha. \quad (A13)$$

This is obviously the Ohm's law region of current. The approximations (A13) are very accurate for  $\alpha < 0.2$ .

Comparing (A12) (upper sign) with (A13) we see that a good estimate for the transition point from Ohm's law to Child's law is  $\alpha \simeq \frac{1}{2}$  corresponding to  $V_a^{(Q-C)} = (ea^2/2\epsilon)\tilde{n}$  as in Fig. 2.

(ii) *The trap-filled crystal (The traps-filled-limit law).*—The threshold voltage  $V_a^{(TFL)}$  of Fig. 2 corresponds to  $\alpha = \frac{1}{2}$ . At voltages slightly above threshold, i.e., for

$\alpha - \frac{1}{2} \ll 1$ ,  $u_a \gg 1$  and the approximations (A8) (lower sign) are valid. The field intensity varies linearly with distance, and the potential parabolically, corresponding to a constant excess charge density  $e(N_t - \bar{n}_t - \bar{n})$ . In this range of voltages the following analytic approximations are useful (note that  $\alpha_t - \frac{1}{2} = (V_a - V_a^{(\text{TFL})}) / 2V_a^{(\text{TFL})}$ ):

$$J \sim \frac{2(\alpha_t - \frac{1}{2})}{\ln[1/(\alpha_t - \frac{1}{2})] + \ln \ln[1/(\alpha_t - \frac{1}{2})] - 1}; \quad (\text{A14})$$

$$J \sim \frac{e\bar{n}\mu}{a} \frac{(V_a - V_a^{(\text{TFL})})}{\ln[V_a^{(\text{TFL})}/(V_a - V_a^{(\text{TFL})})]} \quad (\text{A15})$$

$$\frac{n_a}{\bar{n}} \sim \frac{(\alpha_t - \frac{1}{2})}{\ln[1/(\alpha_t - \frac{1}{2})]}; \quad \frac{\mathcal{E}_a}{\mathcal{E}_\Omega} \sim 2.$$

The "verticality" of the  $J-V$  curve for the traps-filled-limit case for  $V_a$  near threshold,  $V_a^{(\text{TFL})}$ , follows from (A14).

To establish the size of the error made by substituting  $n_a$  for  $n_\Omega = (1/a) \int_0^a n(x) dx$ , we note that integration of Eq. (A1) (lower sign) gives  $e\mathcal{E}_a/ea = n_\Omega + \bar{n}$ . For  $\alpha_t - \frac{1}{2} \ll 1$ ,  $\mathcal{E}_a$  may be replaced by  $2\mathcal{E}_\Omega$  from (A15). From (A9) and (A15):

$$(\alpha_t - \frac{1}{2} \ll 1); \quad \frac{n_a}{\bar{n}} = 2(\alpha_t - \frac{1}{2}), \quad (\text{A16})$$

$$\frac{n_a}{n_\Omega} \approx \frac{1}{2 \ln[1/(\alpha_t - \frac{1}{2})]}.$$

Since  $n_a/n_\Omega \rightarrow 0$  as  $\alpha_t \rightarrow \frac{1}{2}$ , it follows that it is impossible to establish a general inequality, along the lines of (8), confining  $n_a$ , within relatively narrow limits, near  $n_\Omega$ .

The simplified arguments of Sec. IV, namely Eqs. (9) and (10), applied to the traps-filled case give the result

$$(V_a - V_a^{(\text{TFL})}) / V_a^{(\text{TFL})} \ll 1: \quad J \approx (e\bar{n}\mu/a)[V_a - V_a^{(\text{TFL})}]. \quad (\text{A17})$$

The difference voltage,  $V_a - V_a^{(\text{TFL})}$ , appears in (A17) instead of  $V_a$  alone as in Eq. (10), because in the TFL case  $\mathcal{E}(0) \neq 0$  until  $V_a \geq V_a^{(\text{TFL})}$ . Comparing the  $J_{\text{approx}}$  of (A17) with the  $J_{\text{exact}}$  of (A14), we have

$$\frac{J_{\text{exact}}}{J_{\text{approx}}} \approx \left\{ \ln \left[ \frac{V_a^{(\text{TFL})}}{(V_a - V_a^{(\text{TFL})})} \right] \right\}^{-1}.$$

It may be concluded then, that, except for the case that  $(V_a - V_a^{(\text{TFL})}) / V_a^{(\text{TFL})}$  is very small indeed, the approximation (A17) is correct within a factor of two or three. Since for the real crystal,  $n_a < \bar{n}$  is impossible, it is in any case, not physically sensible to take  $(V_a - V_a^{(\text{TFL})}) / V_a^{(\text{TFL})} \ll 1$  in the argument of the above logarithm. Since we would expect that the greatest

error arising from the approximation  $n_a \approx n_\Omega$  occurs precisely in the TFL case, we conclude quite generally that this approximation, and its companion  $n_{ta} \approx n_{t\Omega}$ , do not lead to errors of more than a factor of two or three.

#### APPENDIX B. INSULATOR WITH "SHALLOW" TRAPS

Electron traps at a given location in an insulator are said to be "shallow" if they lie, energetically, above the steady-state Fermi level for electrons at that position. The property of being "shallow" is clearly not an intrinsic property of the trap, but depends both on the degree of excitation of the insulator and on the temperature. We have already seen, in the discussion of Sec. IV, that if the traps are shallow then there is a fixed ratio  $\theta$ , independent of applied voltage, between  $n$  and  $n_t$ . For a discrete trap level,  $\theta$  is given by (11). Assuming that  $\theta \ll 1$ , at distances sufficiently removed from the cathode (in the simplified theory  $n = \infty$  at the cathode requires that all traps be filled near the cathode), Eq. (2) can be written

$$(\theta\epsilon/e)(d\mathcal{E}/dx) = n - \bar{n}. \quad (\text{B1})$$

An appropriate set of dimensionless variables for the description of the solution in this case is obtained simply by replacing  $\epsilon$  by  $\theta\epsilon$  in (A1), (A2), and (A9):

$$w_\theta = \frac{1}{\theta} w, \quad u_\theta = u, \quad v_\theta = \frac{1}{\theta} v, \quad \alpha_\theta = \theta\alpha = \frac{v_{\theta,a}}{w_{\theta,a}^2}. \quad (\text{B2})$$

The results (A12) and (A13) are now valid with  $\alpha$  replaced by  $\alpha_\theta$ . The transition point from Ohm's law to Child's law is  $\alpha_\theta \approx \frac{1}{2}$ , corresponding to the transition voltage  $V_{\theta,a}^{(\Omega-\epsilon)} = e a^2 \bar{n} / 2\epsilon\theta$ . From the relation  $J/J_\Omega \simeq 9\alpha_\theta/8$ , valid for  $\alpha_\theta \gg 1$ , is obtained the modified Child's law,  $J = 9\theta\epsilon\mu V_a^2 / 8a^3$ . This modified Child's law is often described by referring to a "reduced effective mobility"  $\mu_\theta = \theta\mu$ . In our opinion this is not an appropriate description since, for example, it fails completely to describe the modified transition voltage  $V_{\theta,a}^{(\Omega-\epsilon)}$ , which does not involve the mobility. Mathematically, the above discussion indicates that it would be more appropriate to define a "reduced effective dielectric constant"  $\epsilon_\theta = \theta\epsilon$ . Physically, however, this does not have much significance.

#### APPENDIX C. MATHEMATICAL SOLUTIONS FOR AN INSULATOR WITH A SINGLE DISCRETE TRAP LEVEL

The equations to be integrated are (1), (2), and (4), the last being the equation of state for a single, discrete level. Letting  $M = \bar{n} + \bar{n}_t$ , the solution is conveniently expressed in terms of the dimensionless variables  $\omega$ ,  $\lambda$ , and  $\varphi$  defined in direct analogy with the variables  $w$ ,  $u$  and  $v$  respectively of (A2)

$$\omega = e^2 M^2 \mu x / \epsilon J; \quad \lambda = e M \mu \mathcal{E} / J = M/n; \quad \varphi = e^3 M^3 \mu^2 V / \epsilon J^2. \quad (\text{C1})$$



The equation of state (4) can be rewritten

$$n_i/M = c/(1+b\lambda), \text{ with } c = N_i/M, \text{ } b = N/M, \\ N = N_c \exp[(E_i - E_c)/kT]. \quad (C2)$$

The Poisson equation (2) becomes

$$\frac{d\lambda}{d\omega} = \frac{1-\lambda}{\lambda} + \frac{c}{1+b\lambda}; \quad \omega = \int_0^\lambda \frac{\lambda(1+b\lambda)}{(1-\lambda)(1+b\lambda)+c\lambda} d\lambda. \quad (C3)$$

For the potential,

$$\varphi = \int_0^\lambda \frac{d\omega}{\lambda} = \int_0^\lambda \frac{\lambda^2(1+b\lambda)}{(1-\lambda)(1+b\lambda)+c\lambda} d\lambda. \quad (C4)$$

The range of  $\lambda$  is from  $\lambda=0$  at  $\omega=0$  to  $\lambda=\lambda_{\max} = M/\bar{n}$  at  $\omega = \infty$ .

Equations (C3) and (C4), subject to the boundary condition (7):  $\lambda=0$  at  $\omega=0$ , are directly integrated by the use of partial fractions. It is convenient to express the results in terms of the new "normalized" dimensionless variables  $\Omega$ ,  $\Lambda$ , and  $\Phi$  defined by

$$\Omega = \omega/\lambda_{\max}, \quad \Lambda = \lambda/\lambda_{\max}, \quad \Phi = \varphi/\lambda_{\max}^2. \quad (C5)$$

The final equations, without any approximations, are

$$\Omega = -\Lambda - \frac{\alpha}{2} \ln \left\{ 1 + \frac{2}{\delta} (1+\eta)\Lambda(1-\Lambda) - \Lambda^2 \right\} \\ + e \ln \frac{1+\eta}{1-\Lambda} \quad (C6)$$

$$\Phi = -\frac{1}{2}\Lambda^2 - \alpha\Lambda - \mathcal{D} \ln \left\{ 1 + \frac{2}{\delta} (1+\eta)\Lambda(1-\Lambda) - \Lambda^2 \right\} \\ + \mathcal{F} \ln \frac{1+\eta}{1-\Lambda} \quad (C7)$$

with

$$\delta = 1/2bB_0^2; \quad B_0 = (c+b-1)/2b; \quad \eta = \frac{1}{2}\{(1+2\delta)^{\frac{1}{2}} - 1\}; \\ \alpha = \frac{2bB_0+1}{2bB_0(1+\eta)}; \quad e = \frac{\alpha}{2(1+2\eta)} + \frac{\delta}{2(1+\eta)(1+2\eta)}; \\ \mathcal{D} = \frac{\alpha}{2(1+\eta)} + \frac{\delta}{4(1+\eta)^2}; \\ \mathcal{F} = \frac{(1+\delta)\alpha}{2(1+\eta)(1+2\eta)} + \frac{\delta}{4(1+\eta)^2(1+2\eta)}.$$

The results (C6) and (C7) and the accompanying expression for the coefficients can be expressed in an algebraically more compact form. However, the above form is one which the author has found particularly suitable for actual calculations. Underlying the choice of this form is the fact that  $\delta \ll 1$ , whence  $\eta \simeq \frac{1}{2}\delta(1 - \frac{1}{2}\delta)$ , in cases of particular interest, such as those plotted up in Fig. 5. In analogy with (A9), a new dimensionless parameter  $\alpha_M$  is defined

$$\alpha_M = \epsilon V_a / e M a^2 = \Phi_a / \Omega_a^2. \quad (C8)$$

$J$ ,  $n_a$ , and  $\mathcal{E}_a$  are determined from

$$J/J_\Omega = \Omega_a / \Phi_a; \quad n_a/\bar{n} = 1/\Lambda_a; \quad \mathcal{E}_a/\mathcal{E}_\Omega = \Lambda_a \Omega_a / \Phi_a. \quad (C9)$$

Each portion of the  $J-V$  characteristic is associated with a definite range of  $\Lambda$  in Eqs. (C6) and (C7). This detailed association is listed in Table I. For each range

TABLE I. The ranges of  $\Lambda$  associated with the different portions of the  $J-V$  characteristic for a single, discrete trap level.  $\delta = 1/2bB_0^2$ ,  $\zeta = B_0\delta$ ,  $B_0 = (c+b-1)/2b$  [see (C2)].<sup>a</sup>

Range of $\Lambda$	Associated portion of the $J-V$ characteristic
1 to 0.97	Ohm's law
0.97 to 0.1	Transition
0.1 to $10\zeta$	Modified Child's law
$10\zeta$ to $0.1\zeta$	Transition
$0.1\zeta$ to $10\delta$	Traps-filled-limit law
$10\delta$ to $\delta$	Transition
$\delta > \Lambda$	Child's law

<sup>a</sup> If the values of  $\delta$  and  $\zeta$  are such that one of the ranges listed for  $\Lambda$  is not available, then the corresponding portion will be missing from the  $J-V$  characteristic.

of  $\Lambda$  appropriate simplifications of Eqs. (C6) and (C7) are readily worked out.